SYNTHESIS REPORT

FOR PUBLICATION

CONTRACT N°: BREU CT91-0400

PROJECT No: BE-4249-90

TITLE: DEVELOPMENT OF A NEW GENERATION OF ARTIFICIAL HIP JOINTS CONTAINING COMPLIANT LAYERS

PROJECT COORDINATOR:

DR J D BOLTON
UNIVERSITY OF BRADFORD **UK**

PARTNERS:

UNIVERSITY OF BRADFORD **UK**

UNIVERSITY OF DURHAM **UK**

UNIVERSITY OF LIMERICK **IRL**

ARMINES/ÉCOLE DES MINES DE PARIS F

STARTING DATE: 01.09.91 DURATION: 60 MONTHS

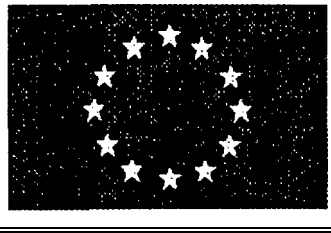

PROJECT FUNDED BY THE EUROPEAN COMMISSION UNDER THE BRITE/EURAM PROGRAM

DATE: 01.09.1996

DEVELOPMENT OF A NEW GENERATION OF ARTIFICIAL HIP JOINTS CONTAINING COMPLIANT LAYERS

B. S. Becker', V. Barron[2], C. Birkenshaw[2], J.D. Bolton[1], K. J. Bryan[2], M.Bugg[2], 1. C. Burgess[3], J. L. Cunningham[3*], A. E. P. Morris[4], T.V. Parry[3**], F. Quigley[2], M. E. R. Shanahan[4], A. Unsworth[3], & J. Q. Yao[3***]

1. Dept. of Manufacturing and Mechanical Engineering. University of Bradford, Bradford, BD7 DP, UK.
2. Dept. of Materials Science and Technology, University of Limerick, Limerick, Ireland
3. School of Engineering and Computer Science, University of Durham, Durham. DH 13LE, UK * until 7/9S, **until 9/94, *** until 1 1/94
4. Centre des Materiaux Pierre - Marie Fourt, Ecole des Mines de Paris, BP 87,91003 Evry Cedex, France

ABSTRACT

The incorporation of impervious elastomeric compliant layers onto the surface of acetabular cups was known to generate fluid film lubrication conditions. Friction levels comparable to those of healthy human joints have been observed, with the surfaces of the joint remaining separated under a wide range of simulated human activities. Long term wear resistance of artificial hip joints could therefore be substantially improved, increasing the average prosthesis lifetime from 10 years to 25 years or more. However, poor adhesion between (fully dense) stainless steel substrates and the elastomer prevented any further exploitation of this system.

The work outlined in this paper investigates the fixation of biocompatible elastomers to porous metal substrates produced by powder metallurgy and the development of heterogeneous polymeric systems with compliant surfaces. Powders of approved biocompatible metals were processed to give prototype porous components, enhancing adhesion by the mechanical interlocking of the elastomeric layers, whilst a parallel route investigated the potential of using polymeric substrates by developing a novel bonding technique. A multi-station hip function simulator, specifically designed for this project, was then used to study the fiction and wear behaviour of prototype acetabular cups using the compliant layered bearing systems developed.

INTRODUCTION

The human hip is a ball and socket joint and is one of the largest and most heavily loaded joints in the body. If this joint is affected by arthritis, and particularly osteoarthritis where degradation of the cartilage results in rubbing of bone ends, the resulting pain and stiffness can severely restrict a patients' mobility. Charnley [1] pioneered the Total Hip Replacement (THR) prosthesis in the 1960's using a stainless steel femoral stem with a 22rnm diameter head articulating against a polymeric acetabular component manufactured from Ultra High Molecular Weight Polyethylene (UHMWPE). Currently world-wide, 500,000 THR's are performed each year, for which a clinical success rate of 90°/0 is claimed for patients over 65 years of age. Successful joints are defined in terms of the lifetime of the THR before a revision (repeat) operation is required. Despite some Charnley joints lasting in excess of 20 years [2], the average accepted lifetime for patients aged 65 years or more is ten years. However, younger patients between 16 and 40 years old are generally more active and therefore average THR lifetimes can drop to three years. This together with the limitation that only three THR's can be implanted during an average person's lifetime, often prevents these patients from being considered for this operation.

The majority of hip replacement failures are associated with stem/cup loosening or infection, with a smaller but significant number of revision operations being required because of wear [3]. Loosening of the femoral component has now been attributed to adverse tissue reactions to the UHMWPE wear debris, causing, bone necrosis around the implant. A small number of THR's fail due to bone resorption from a different source, which occurs as a result of the reduced force experienced by the cortical bone following the insertion of a femoral stem made from a stiffer material. In some treatment centres 25% of the annual work load consists of revision operations [4] which is set to increase unless low fiction joints with longer useful lives can be developed. Such a development would also reduce orthopedic surgery workloads, costs and enable younger patients to benefit from this surgical procedure.

Recent attempts to minimise the risk of hip joint loosening have developed in four main directions: 1) the use of low elastic modulus implants, where work has concentrated on developing new titanium alloys [5,6,7], 2) improving the properties of bone cements [8,9], 3) biological fixation using porous implant coatings to encourage cortical bone ingrowth and 4) to reduce the problem of wear, harder prostheses have been developed, either by incorporating intrinsically hard materials - such as alumina ceramics - into the joint design [10,1 1,12], or by surface modification - such as ion nitriding [13,14]. However, although' this approach may 'initially appear to be a logical one, this is not the solution adopted by nature.

Articular cartilage has a sot? load bearing exterior comprising of collagen fibres that run parallel to the surface. Unsworth and co-workers [15,16,17] have demonstrated that the low friction levels and wear rates associated with healthy human joints arise from fluid film lubrication. This means that the moving surfaces of the joint remain separated by a continuous layer of synovial fluid which is linked to the compliance of the cartilage surface. Unsworth [18] has also shown that all currently available artificial joints operate in a mixed lubrication regime, where the joint loads are carried directly by metal/plastic contacts with inevitably high friction levels and wear rates. From this research a prototype acetabular cup was developed where the dense metal bearing surface was

covered with a soft elastomer. Friction levels comparable to those of healthy human joints were recorded for this technology [17], i.e. f = 0.001, which is one order of magnitude lower than any currently available prosthesis. Furthermore, the bearing surfaces were found to remain separated from one another even when lubricated with low viscosity (diseased) synovial fluid. A ten fold reduction in the viscosity of synovial fluid is characteristic of osteoarthritis, therefore the adoption of this technology could significantly increase the long term wear capabilities of THR's.

Immediate commercialisation of this product was prevented by the poor mechanical integrity achieved at the metal/polymer interface, which was found to break down after approximately 100, 000 cycles on a hip joint simulator [18] plus the polymer was found not to be biostable. Therefore, the adhesion between the layer and the substrate limited the useful life of this novel type of joint. The major objective of this work was to develop low friction (typically μ = 0.004), wear resistant, biocompatible and biostable acetabular cups containing compliant layers for articulating against conventional femoral components offering substantially improved lifetimes of 25 years or more.

Two different routes were used in an attempt to overcome bonding problems:

(l) Impregnating biocompatible elastomers into porous biomedically approved metal substrates produced using powder metallurgy techniques, thereby enhancing the bond adhesion via the mechanical interlocking of the elastomeric layer.

(2) Chemically bonding biocompatible elastomers to polymeric substrates producing heterogeneous polymeric acetabular cups.

TECHNICAL DESCRIPTION

This project involved four academic institutions, where each site concentrated on a specific task, although some parallel work was undertaken. The University of Durham designed the compliant layer cup using numerical mathematical modelling and undertook wear and friction studies on the prototype cups. Processing parameters for the porous metallic substrates, produced by powder metallurgy techniques, were developed at the University of Bradford and realised at Manganese Bronze Components Ltd. Suitable polymers for the compliant layer were identified and characterised by the University of Limerick, who also undertook finite element analysis of a three dimensional hemi-pelvis and developed polymeric substrates and suitable bonding techniques for the heterogeneous polymeric acetabular cups. Finally, the interracial properties of the metal/polymer bond were characterised and , modelled by École des Mines de Paris. Each of the industrial endorsers played a significant role within the project offering facilities and know-how; Scientific Metal Powders Ltd supplied water atomised Co-29Cr-6Mo powders, while Manganese Bronze Sintered Components Ltd provided the tooling design and hydraulic presses required to manufacture the prototype cups. Finally, Howmedica International Inc. gave constant advice on all aspects of the project and provided facilities for injection moulding the compliant layer into the acetabular cups. Howmedica International Inc. also manufactured the 'novel surfaced' prototype cups.

A mathematical analysis of the elastohydrodynamic lubrication (EHL) performance due to the entraining action was conducted using empirical numerical procedures capable of solving the governing elasticity and viscous flow equations for point contact conditions. A new numerical method to solve the problem was developed based on the Newton linearisation of a non linear integral-differential system equation, coupled with a composite direct-iterative linear solver, with the cavitation condition satisfied during the solution of the linear matrix equation. This theoretical model of compliant layer lubrication identified the important parameters required for the prototype acetabular cups, such as layer thickness, layer modulus, and the modulus of the backing substrate. The effect of these parameters on the stress levels in an anatomically correct hemi-pelvis were modelled by the University of Limerick using Finite Element Analysis (FE). The resulting model supported the numerical analyses and determined the nature of the stresses experienced by the subchondral bone following implantation. Three dimensional pelvic geometry was obtained from CT scans of a male human pelvis. Using mesh generating software the polylines obtained from the CT scanner were built into a solid model of the right hemi-pelvis which was meshed to form the finite element model. Three-dimensional solid brick elements were" used to represent the trabecular bone while the cortical shell was represented by variable thickness shell elements which were added gradually until the complete model was constructed. The joint load- was taken as 2 160N, which occurs at the beginning of the single legged stance phase, representing the worst case of loading during normal walking. Corresponding muscle loads at the same instance in the walking cycle were also added [19,20].

A number of elastomeric materials were reported, by their manufacturers, to be suitable for biomedical applications, but many of these claims were unsubstantiated. A comprehensive, database of biocompatible elastomers was generated which included polyurethane as well as silicones and experimental polymers. The most appropriate compliant layer materials were then chosen after a lengthy materials selection exercise had been carried out where the physical and the mechanical properties of the various polymers were characterised in terms of biostability, biocompatibility and tribological properties.

The molecular structure and mechanical properties of the elastomeric materials both before and after hygrothermal ageing (for periods up to 2 years in either distilled water or Ringer's Solution at 37°C) or irradiation

(using a Cobalt 60 source at a dose rate of 0.156Mrad-' to two dosages of 2.5 Mrad or 5.0Mrad) were characterised using Differential Scanning Calorimetry (DSC), Dielectric Thermal Analysis (DETA), Dynamic Mechanical Thermal Analysis (DMTA), and more sophisticated techniques of Gel Per neation Chromatography (GPC) and Infrared Spectroscopy. Mechanical testing of the polymers consisted of Shore hardness testing and compression fatigue testing, using an in-house facility, adapted for use with both flat elastomeric samples and compliant acetabular cups 'in situ'. Fatigue testing was performed at frequencies of either 1.5Hz or 10HZ between O and -2.5MPa, at ambient temperatures or 37°C, and either dry or in Ringers Solut on after equilibrating the polymers in the relevant condition before testing.

The possibility of producing porous metal substrates from metal pow ders of water atomised 3 16L stainless steels, water atomised Co-29Cr-6Mo alloy plus a novel bimodal Co-29Cr-6Mo powder (manufactured by dry blending 50 wt % of coarse water atomised powder with 50 wt % of ball milled gas atomised powder) and blended elemental Ti-6Al-4V powders was investigated. The processing parameters. corrosion behaviour and mechanical properties were established for each of the four metal powders. Each powder was sieved into seven different fractions, except for the bimodal Co-29 Cr-6Mo powder, of 'which three were chosen for further study: a coarse size, an intermediate size and a fine size. Porous materials were produced over a range of porosity by varying four parameters: the initial powder particle size, the compaction pressure (b etween 154- 1235MPa), the sintering temperature (between 1100- 1350"C) and the sintering atmosphere (vacuum, flowing argon and flowing molecular 75%H_2/25%N_2). Ti-6Al-4V alloys were only sintered under vacuum, but s elected samples underwent a gaseous surface nitriding treatment. After sintering, densities and porosity character sties were determined using a xylene impregnation method adopted from ASTM Standard B378-73, [21].

For each material the mode of sintering was determined by microstructural analysis using both optical and scanning electron microscopy and by micro-analytical analysis using Energy Dispersive X-Ray Analysis (EDAX). Quantitative image analysis (QIA) was used to characterise the pore shape and size, which were related to the corrosion behaviour of the porous materials. from both potentiodynamic anodic polarisation tests (conducted at a sweep rate of 12mV/s from -1 .5V to +1 .5V in 0.2M KCL solution at 37 ±1 'C) and long term open circuit tests (conducted in either 0.2M KC1 solution or Flank's Solution [22] both aerated and de-aerated at 37 ± l°C for 100 hours) and to the mechanical properties determined from apparent hardness, compression and tensile testing.

École des Mines/Armines aIso conducted hygrothermal ageing experiments on the candidate materials (by exposing the polymers to distilled water and ¼ Ringers Solution at 40°C and 55°C) and characterizing.the molecular ,. changes in the polymer using DSC, complementing the work undertaken by the University of Limerick. Furthermore, pore geometry of the porous metallic substrates was characterised using QIA and scanning electron microscopy generating further data to support the work undertaken at Bradford University. But their essential role was to determine the best method of bonding the elastomer to the metallic substrate using a variety of sample surfaces (from sintered samples of various porosity provided by the Univers ty of Bradford and Manganese Bronze Sintered Components Ltd to "novel" surfaces supplied by Howmedica International Inc.) and hot compression moulding and then testing the mechanical integrity of the bond using torsional test equipment developed specifically for this project, based on a modified Napkin Ring test [23].

The long term wear and fiction tests, which were essential to assess the performance of the prototype compliant layer acetabular cups, were undertaken by the University of Durham using a five-station hip joint simulator and an in-house fiction machine. The latter was used to establish if the cups were performing under fluid film conditions thereby providing experimental data to support the developed theory. The hip simulator was specifically designed, constructed and commissioned as part of the project and simulated, three degrees of freedom, (vertical, flexion-extension and pelvic rotation) at a frequency of 1Hz (equivalent to walking pace). Prior to this machine being used to undertake wear studies of the prototype cups up to 1 million cycles, a validation exercise was undertaken using both UHMWPE cups and PTFE cups. The results obtained were compared to the known literature [24-29] and were found to be broadly similar. Testing of the prototype cups was undertaken until the cups were deemed to have failed, when either extensive debonding of the layer from the substrate or extensive wear of the bearing surface was noted. The performance of the cups was then assessed by visually examining the cups for evidence of bearing wear, debonding, corrosion and creep and by determining the surface topography of both the heads and cups using a Zygo non-contacting pro kilometer.

RESULTS

Modelling the CUP Design

The numerical modelling derived two empirical equations:

$$h_{cen} = -\frac{7.410\, h_t^{0.670} (\eta u)^{0.660} R^{0.543}}{E'^{0.221} w^{0.437}} \quad (1)$$

$$h_{min} = 6.460\, h_t^{0.670} \frac{(\eta u)^{0.660} R^{0.543}}{E^{0.223} w^{0.467}} \quad (2)$$

where: h_{cen} = central lubricant film thickness (m); H_{min} = minimum lubricant film thickness (m); h_t = thickness of compliant layer (m); R = equivalent radius (m) = $R_1 . R_2 / R_2 - R_1$ (R_1 = radius of the femoral head (m) and R_2 = radius of the acetabular component (m); E = elastic modulus of the compliant layer (Pa); η = viscosity (Pa s) u = entraining velocity (ins-') and w = applied load (N).

From the above analyses, it can be shown that in order to increase h_{cen} and h_{min} increasing h_t is more influential than increasing R, which was more influential than decreasing E.

Furthermore, pure squeeze film lubrication was aiso examined. A formula predicting the film thickness was developed for a thin incompressible layer bonded to a rigid substrate, and is given below.

$$h = 6.655 \left(\frac{h_t^6 R^2 \eta^3}{w t^3 E^3} \right)^{K} \quad (3)$$

These results were particularity noteworthy since they allowed a parametric analysis of the effect of various design parameters such as Youngs' Modulus, the equivalent radius, the roughness of the compliant layer, and the minimum film thickness required to be evaluated, fundamental to the design of compliant layer THR's.

When the above analyses were applied to natural synovial joints, d-u: predicted film thickness was at best similar in size to the surface roughness of the articulating surfaces. However, pressure perturbations in the lubricant developed due to the entraining action of the surface asperities which effectively smoothed them and sustained film thicknesses less than those predicted by the smooth case analysis discussed above. This mechanism is known as micro-elastohydrodynamic lubrication (μ-EHL) or asperity lubrication. A new theory of asperity lubrication was developed which expiored the effects of different types of surface roughness [30,31]. This theory was found to be equally applicable to compliant layered joints, and therefore was used as a guideline for the prototype design.

Contact analysis was essential to provide base data on the required bonding strength of the layer substrate interface, the stress distribution in the layer and it's substrate, and the contact pressure in the joint. An accurate method of predicting these parameters was deveioped [32] and applied to the design of the acetabular components [33]. In particular, design charts and power law formulae were developed which allowed the contact radius and the maximum shear stress to be readily evaluated for a wide range of design conditions. These formulae are given , below.

$$a = 0.94 h_t^{0.38} \left(\frac{wR}{E} \right)^{0.21} \quad (4)$$

$$\tau_{max} = 0.22 \left(\frac{w^{0.52} E^{0.48}}{h^{0.56} R^{0.48}} \right) \quad (5)$$

The above analysis showed that the maximum shear stress which usually occurred at the bonding interface, is of the order of 1 MPa, and hence the most likely failure mode will be failure at the layer substrate interface. The effect of the lubrication regime on the contact stresses was also evaluated. When the fiction between the articulating surfaces was low (i.e. μ<0.0 1- fluid film lubrication) the lubrication regime had a negligible effect on the stress field, and hence debonding of the compliant layer was still the most likely failure mode. However if the fiction between the articulating surfaces was high (i.e. μ>0. 1- surface contact) the effect on the: tress field was more pronounced. The maximum shear stress increased and was found to be at the beating surfaces, and hence the most likely failure mode became cohesive failure of the compliant layer. These results illustrated the importance of designing for fluid film lubrication, with layer adhesion capable of withstanding maximum shear stresses in excess of 1 MPa.

Finite Element modelling of the compliant layer using both 2- dimensional models and 3-dimensional models also showed that the maximum shear stresses would be at the metal/ polymer interface. The work was then extended to consider the effects of implanting a rigid acetabular implant on the pelvic and subchondral bone or cement stresses. This showed that using either a rigid metallic substrate or a hard polymeric substrates such as carbon fibre reinforced polymers resulted in relatively high stress transfer to the superior rim of the acetabulum (see Figure 1). Using a "flexible" acetabular cup consisting of two iow modulus compliant layers (so that the combined modulus was iess than 20GPa) gave stresses in the subchondral bone identica I to that of the natural joint. (see Figure 2 & 3). The FE work combined with concerns about the corrosion resistance of the stainless steel metal shells ied to the parallel work on heterogeneous polymeric cups.

The Compliant Layer

Previous work on fluid film lubrication had indicated that polymeric materials with a hardness in the range of 3.5 - 9 Nmm^{-2} H20/30 (DIN 53456) can yield tribological properties that promote hydrodynamic lubrication of compliant bearings. This fundamental constraint enabled the initial selection of elastomeric polymers from materials which had some degree of biomedical history. Therefore an initial set of evaluation criteria for the compliant layer

was as follows: 1) hardness between 80°A and 85°A (Shore A Scale), 2) initial modulus in the range 20-30 MPa, 3) biocompatibility - at minimum must satisfy USP XXII class 6, 4)evidence of biostability, 5) resistance to hydrolysis, 6) low compression set and hysteretic loss, i.e. below 20'% of thickness at at 23°C and 25% strain, and 7) good fatigue life, i.e. the polymer must not fail while being cycled at 10 Hz for 1 million. cycles.

Around thirteen different polymeric materials formed the initial list of candidate materials consisting of nine mainstream polyurethane, including Estanes and Tecothanes, two silicon urethanes including C-Flex and 2 research materials: Hexsyn and Rimplast PYUA.

Elastomeric polyurethane appeared to satisfy many of the requirements largely because of their multiphase morphology. These materials can be typically defined as linear block copolymers of the (AB)n type, where one block of the polymer chain consists of a relatively long soft segment, - the macroglycol, as derived from a hydroxyl terminated polyether with a molecular weight in the range 1000-2000 Daltons. The second, highly polar and stiff block of the copolymer, commonly referred to as the hard segment, is formed by the reaction of isocyanates with low molecular weight diols or diamine chain extenders. The properties of these materials are significantly influenced by the monomers used for the synthesis of the polymers an i the stoichiometric balance of the components along with molecular factors such as intermolecular forces, chain flexibility and conformation of both the hard and soft segments.

The thirteen materials were then evaluated using, experimentally determined properties detailed in Table 1, which were then compared and ranked to the initial evaluation criteria listed above. This exercise resulted in three possible compliant layer candidates being identified: Tecothane 1085A, Tecothane1 095A and Estane 5714F1. Hygrothermal ageing and irradiation studies were now conducted to optimise the material choice.

During the first three weeks of hydrothermal ageing in distilled water and in Ringers Solution, the Estane materials exhibited considerable mass uptake. Longer term hydrothermal ageing resulted in weight loss due to the leaching of processing agents and stabilisers as well as molecular degradation through hydrolysis, resulting in the degradation of mechanical properties. However, the Tecothanes displayed a much improved stability with no substantial loss in mechanical properties or phase segregation.

Irradiation results had a similar trend, although the differences between the Estane and the Tecothane materials were not so marked. Both exhibited shifts in the DMTA curves and increases in tensile properties due to chain entanglements between the phases restricting the molecular vibrations within the soft segments, which became more marked at the higher dosage.

Fatigue testing flat specimens of both the Tecothanes and the Estanes dry resulted in appreciable hysteresis, which reduced significantly as loading continued, marking the onset of compression set, (see Figure 4). Concurrently a large increase in the dynamic modulus was noted. The Tecothanes displayed higher dynamic moduli compared to the Estanes suggesting that Tecothanes undergo less creep. Testing the Tecothanes in Ringers Solution at 37°C reduced the peak modulus, (see Table 2) and therefore greater compression sets were exhibited - indicating that the samples had softened (see Figure 5). After irradiation, higher peak moduli were recorded, which were in line with the DMTA results indicated above. Fatigue testing of the prototype cups containing a compliant layer showed similar results to the flat specimens, the only difference being that delamination at the polymer/substrate bond resulted in a significant shift of the hysteresis curve to the left, (see Figure 6). DSC work following the fatigue tests indicated that segmented polyurethanes do not undergo significant structural alterations during fatigue, and generally had good integrity when loaded to the stress levels experienced in hip joints.

Manufacturing the Metal or Polymer Substrate

Metallic substrates were initially fabricated from 3 16L stainless steel powders, even though this material was known to have inferior corrosion resistance compared to either of the other biomedically approved alloys, Co-Cr-Mo or Ti-6Al-4V, because: 1) commercial knowledge of this material in both the wrought and powdered state dated from the" early 1950's, 2) the raw material was inexpensive and readily available and 3) the amount of compact shrinkage during sintering was predictable and controllable. Throughout the project, stainless steel was used as a "control" material to which the other two materials were compared, even though it had been eliminated as a candidate for the final product. See Table 3 for baseline compositional information.

Porous metallic substrates were fabricated with a maximum range of total porosity, for each material, between 4-35% and a maximum interconnected range of O. 1-30%. Different sintering mechanisms were observed for each material affecting the closed to interconnected porosity ratio and changing the pore morphology over the porosity range; 3 16L stainless steels sintered by solid state diffusion whilst both Co-29Cr-6Mo and Ti-6Al-4V alloys exhibited a transient liquid phase. This was particularly noticeable in argon sintered, water atomised and bimodal Co-29 Cr-6Mo powders as carbide eutectics formed above 1300°C. ~116L stainless steels therefore exhibited a uniform and well distributed network of pores with a consistent pore geometry, provided that only one particle size was used. The Ti-6Al-4V alloys were at the other extreme, as the titanium sponge powder particles did not completely close on sintering, giving pore sizes that varied considerably across. the sample with no consistent distribution and considerable variation in pore geometry, (see Figure 7(D)) Both bimodal and water atomised Co-

‘ 29 Cr-6Mo powders had a less variable pore distribution and geometry than the 3 16L stainless steels but were more consistent than the Ti-6Al-4V alloys.

Sintering both 3 16L and Co-29 Cr-6Mo alloys under vacuum caused carbon and chromium to be lost from the free surface, whilst sintering in molecular 75 °/0 H_2/25%N_2 caused a cellular growth of discontinuous chromium nitride (Cr_2N) precipitates. Such surface compositional differences caused significant differences in the corrosion behaviour for these materials, whilst introducing porosity increased corrosion currents due to increased surface areas. Extensive pitting attack was noted for the vacuum sintered alloys, while severe intergranular attack was evident in the molecular 75%H_2/25%N_2 sintered alloys. No obvious signs of corrosive attack were seen on the Ti-6Al-4V alloys, although increased corrosion currents indicated that low levelion dissolution must be taking place.

Both qualitative evidence from the corroded surfaces and quantitat ve evidence from plotting AE values against porosity (see Figure 8) suggested that the most corrosion resistant material was nitrided Ti-6Al-4V alloys. This was confirmed by open circuit testing where rising transients, indicative of passive film formation, were recorded for this material in all environments.

Mechanical properties, such as apparent hardness, Young’s Modulus, and tensile strength all decreased with increasing porosity and all were significantly below those of the wrought materials because the effective load bearing area had been reduced. This was demonstrated by the fracture surfaces where areas of ductile failure were noted at sites of previous particle-to-particle contact, (see Figure 9). Surface compositional changes in 3 16L and Co-29 Cr-6Mo alloys also affected the mechanical properties. For instance the presence of cellular Cr_2N precipitates increased tensile strength at the expense of ductility, whilst vacuum sintering appeared to improve the ductility at the expense of tensile strength. Gaseous nitrided Ti-6Al-4V alloys, which appeared to give the best corrosion results due to the formation of nitrides around pore edges, failed catastrophically by transcrystalline cleavage fracture originating from these nitrides.

A more important mechanical test was to determine if the porous materials would undergo pore collapse when subjected to physiological loadings. The FE analysis determined that the compressive stresses in the acetabulum were between 35-45MPa. Therefore if a permanent change in shape could be discerned at these stress levels then the porous material would have been deemed to fail. Figure 10 indicates that both 316L and Ti-6Al-4V displayed some permanent plastic deformation in this stress range, although the Ti-6Al-4V samples appeared to perform slightly better.

Overall, a materials selection exercise had been undertaken, for the metallic materials, where all the necessary data had been generated as part of the project, leading to un-nitrided Ti-6Al-4V alloys being identified as the most suitable material for this application:

Sintered prototype metal acetabular cups were manufactured using both 316L stainless steel and the Ti-6Al-4V alloys by Manganese Bronze Sintered Components Ltd, in a double action hydraulic press using tooling designed in-house. The sintered cups were then sent to Howmedica International Inc. where the compliant layer was injection moulded into the metal substrates. (Due to the distortion that occurred when sintering the Ti-6Al-4V cups injection moulding a suitable compliant layer proved impossible). Furthermore, Howmedica International’ Inc. manufactured “novel surfaced” acetabular cups containing macro-porosity which were also injection moulded with the compliant layer. All the metal backed cups were sent to Durham University for both friction and wear testing.

The most suitable polymeric substrate was identified, by literature review, as a carbon fibre reinforced polymer. Prototype acetabular cups were manufactured using a 24 ply laminate formed using matched metal dies. Initially the compliant layer was bonded into the cup using simple compression moulding, but this bond was not capable of supporting a high load, therefore other bonding techniques were developed

Bonding the Compliant **Layer** to either the Metal Substrate or the **Polymeric** Substrate

Hot compression moulding was used to characterise the impregnation behaviour of different polyurethane into the different metallic substrates. Initial trials on small porous samples (tested over the porosity range) indicated: 1) that the Tecothanes were more viscous than the Estanes primarily as the Tecothanes were designed for injection moulding rather than compression moulding, 2) as the intercomected porosity in the metallic samples increased so the depth of penetration increased and 3) as the compression time and applied charge increased so the depth of penetration increased. The processing parameters were then optimised to give consistent results with each material, i.e. 180”C for 10 minutes at a charge of 25kN.

Interfacial fracture energy was established by using two opposing cylinders (adherends) ‘bonded’ together using the compliant layers which were tested to destruction (if possible) using a torsion test machine. The apparent energy of adhesion, W, was determined from:

$$W = \frac{\overline{W}}{\pi r_c^2} = \frac{e}{\pi r_c^3}\int M(\gamma_{max})d\gamma_{max} \qquad (6)$$

where M = applied moment; r_e = outer radius of the joint (m); $\overline{W}$ = total energy required to break the joint (J) and e = thickness of the joint (m).

Therefore the area under the M versus γ_{max} curves was used to estimate the apparent energy of adhesion (which is equivalent to strain energy release rate), for various metal surfaces both sintered and 'novel surfaced'. There was an order of magnitude increase in the fracture energy from the dense metal adherends to the porous sintered adherends to the 'novel surfaced' adherends irrespective of the com pliant layer bonding the surfaces, (see Figure 1 I). This increase was attributed to the extent of mechanical interlocking of the compliant layer into the different metal substrates; as the polymer delaminated from the metal surface, fibrils of polymer formed which were anchored to the metal at one end and to the polymer bulk at the other. As the size of the fibrils or polymer necks increased so the fracture energy needed to extend and break these" fibrils inert ased.

A model of the interracial failure was mathematically derived w hich was in good agreement with the experimental results, (see Figure 12).

$$M = \frac{\pi \tilde{G} \theta r_{ex}^4}{2e} - \frac{\pi (G - \tilde{G}) e^3 \gamma_c^4}{6\theta^3} + \frac{2\pi (G - \tilde{G}) \gamma_c r_{ex}^3}{3} \qquad \text{for } \theta \geq \theta_c \tag{7}$$

where, γ_c = critical value. of strain; G = shear modulus on intact interfac: for $\gamma \leq \gamma_c$ (Pa); $\tilde{G}$ = apparent shear modulus for $\gamma \geq \gamma_c$ (pa); r,. = external radius of the cylindrical joint (m).

Various bonding techniques were used to enhance the reinforced carbon fibre / polyurethane bond, such as solvent, plasma and flame treatments. These treatments roughened the surface, allowing the adhesive to flow into the substrate surface and form around each irregularity. After suitable treatm ent to the polymeric substrate followed by bonding of the compliant layer the bond strength was determined by peel testing in accordance with British Standards BS 903 A21. Figure 13 shows that argon plasma treatment gave the highest bond strengths, although work on the possible degradation of this bond when aged in Ringers Solution was not completed.

Friction and Wear Testing of the Prototype Cups

Only the metal backed prototype acetabular cups were tested for friction and wear characteristics, as the heterogeneous polymeric cups were still under development during the latter stages of the project. Friction levels of the prototype cups both sintered and "novel surfaced" containing a Tecothane 1095A compliant layer indicated that full fluid film conditions were operative, (f<0.01) (see Figure 14), validating the numerical analyses indicated in equations (l-3) and giving friction levels well below those established for current metal-on- plastic joints ($f \approx 0.08$).

The wear results, from the multi-station hip joint simulator - see Figure 15, were not so encouraging.,- Stainless steel sintered cups, injection moulded with both Tecothane 1085A and Tecothane 1095A, failed catastrophically (the layer became completely detached from the substrate) after '54000 cycles and 1.0 million cycle respectively, although prior to failure substantial wear debris was observed m the surfaces of both cups. (see Figure 16). However, the "novel surfaced" backed acetabular cup although pro ducing substantial wear debris had not debonded after 1.0 million cycles. Non-contacting profilometry indicated that the both the bearing surfaces and the femoral heads had become progressively rougher as the test continued suggesting that in the hip joint simulator mixed lubrication was the predominant regime.

CONCLUSIONS

(1) New theoretical analyses of the lubrication and contact mechanics for thin layer, heavily loaded point contacts were developed from which the acetabular cup was designed.

(2) Finite element analysis on a three dimensional model of the hemi-pelvis showed that implanting a low modulus acetabular cup would reduce the stresses experienced by the subchondral bone.

(3) A comprehensive database of biocompatible polymers was. generated and several segmented polyurethane chosen for further study. Hygrothermal ageing, irradiation and fatigue testing suggested that the Tecothane family of polyurethane showed the best biocompatiblity and biostability.

(4) Porous materials improved the interracial bonding between the compliant layer and the metallic substrate by 2-3 fold over dense materials. As a result of the materials selection exercise Ti-6Al-4V was identified as the most promising material for this application despite concerns over pore distributions and notch. sensitivity.

(5) A 5-station hip joint simulator was designed and constructed which simulated three degrees of freedom (vertical, flexion-extension and pelvic rotation). This machine was used to test the prototype cups for wear.

(6) Prototype acetabular cups containing compliant layers were produced using both sintered powder metal substrates and polymeric substrates. Sintered substrate cups demonstrate friction levels of $f < 0.01$, better" than friction levels currently available with metal-plastic systems of f 0.05, although wear rates were still high, attributed to the condition of the femoral heads used to conduct the tests.

REFERENCES

[1] Charnley, J.: *The Lancet.* May *27.1961.1129:1132.*

[2] Wroblewski, B. M., Siney, P. D.: *Clin. Orthop. Rel. Res.* (292). 1993.191-201

[3] Dumbleton;, J. H., Tribology of Natural and Artificial Joints. Tribology Series 3. Ellesmere Science Publishing. 1981.3-14

[4] Bulstrode, C. J. K., Carr, A. Murray, D.: *In*: Joint Replacement in the 1990's: Clinical Studies, Financial Implications and Marketing Approaches. MEP, London. 1992.25-27.
[5] Semlitsch, M., Weber, H., Steger, R.: Proc. 8th World Conf. on Titanium. Bimingham. UK. IoM, London. 2 October, 1995.1742-1759
[6] Ahmed, T., Long, M., Silvestri, J. *et al*: Proc. 8th World Conf. on Titanium. Bimingham. UK. IoM, London. 2. October, 1995.1760-1767.
[7] Ito. Y., *et al:* Proc. 8th World Conf. on Titanium. Bimingham. UK. IoM, London. 2. October, 1995.1776-17s3.
[8] Miyamoto, Y. *et al*: *Biomaterials*. 16(11). 1995.855-860.
[9] Deb, S., *et al*: *Biomaterials. 16(14). 1995.1025-1030* (ck).
[10] Griss, P., Heimke, G., V. Andrian-Werberg, H.F.: *Arch. Orthop. Infal'-Chir. 81.1975.259-266.*
[11] Sedel, L., Nizard, R.S., Kerboull, L., Witvoet, J.: *Clin. Othop. Rel. Res.* (298). 1994.175-183
[12] Kumar, P., Oka, M., Ikeuchi, K., *et al: J. Biomed. Mat. Res.* 25.1991 813-828
[13] Buchanan, R. A., Lee, 1.-S., Williams, J-M.: *J. Biomed. Mater. Res. 24(3). 1990.309-318.*
[14] Lemons, J.E.: Proc. Conf. Ion Implantation and Plasma Assisted Processes. Atlanta, Georgia, USA. 22-25 May 1988.51-60
[15] Unsworth, A., Pearcy M.E.J., White, E.F.T, White G., *In*: Tribology - Friction, Lubrication and Wear. Fifty Years on. MEP, London. II. 1987.715-724.
[16] Unsworth, A., Pearcy, M. J., White, E.F.T., White, G.: *Engineering in Medicine. 17(3). 1988.101-104.*
[17] Unsworth, A: *Proc. Instn. Mech. Engrs. Part H. 205.1991.163-172.*
[18] Unsworth, A, Hall, R. M., Burgess, I. C., *et al*: Wear. 190.1995.226-:31.
[19] Dalstra, M., & Huiskes, R..: *J. Biomechanics. 28(6), 1995,715-724.*
[20] Crowinshield, .R.D., & Brand, R.A.: J. *Biomechanics.14(1 1),* 1981, 803-812.
[21] Raghu, T., Malhotra, S.N., Ramakrishnan, P.: *Corrosion. 45(9). 198!. 698-704*
[22] Hanks, J.H., Wallace, R. E.: *Proc. Sot. Exp. Biol. (Wash). 71.1949. 196"*
[23] de Bruyne, N.A.: Adhesion and Adhesives. (eds) N.A.de Bruyn, R.Houwink. 1951.91.
[24] Dowson, D., Jobbins, B.: *Eng. Med., 17(3), 1988,* 111-117.
[25] Derbyshire, B., Fisher, J., Dowson, D., Hardaker, C., Brummitt, K.: *Med. Eng. Phys., 1994,* 16,229-236.
[26] Saikko, V., Paavolainen, P., Kleimola, M., Slatis, P.: *Proc. Instn. Mech. Engrs., I-1206, 1992, 195-200.* . .
[27] Charnley, J., Kamanger, A., Longfield, M.: *Med. Biol. Eng., 7,* 1969, *31.*
[28] Atkinson, J. R., Dowson, D., Isaac, G. H., Wroblewski, B. M.: *Wear 104, 1985,217-224.*
[29] Wroblewski, B.: *JBJS, 67B, 1985,757-761.*
[30] Yao, J.Q. & Unsworth, A.: *Proc. Inst. Mech. Engrs. H207, 1993,* 245-254.
[31] Yao, J.Q.: *In*: Proc.6tb Nordic Symp. Trib. -NORDTRIB '94. Uppsala, Sweden. 1994, 111-118.
[32] Yao, J.Q.: *Proc. Inst. Mech. Engrs. H208,* 1994, *195-205*
[33] Yao, J.Q., Parry, T.V., Unsworth, A., Cunningham, J.L.: *Proc. Inst. Mech. Engrs.* H208, 1994,206-215

ACKNOWLEDGEMENTS

The work reported in this paper was carried out as part of BRITE/EuRaM project No. BE-4249-90, 'Development of a new generation of artificial hip joints containing compliant layers' funded by the European Union and endorsed by Howmedica International Inc., Manganese Bronze Components Ltd. and Scientific Metal Powders Ltd.

Table 1: Identification of the mechanical property parameters required for a compliant polymer layer and appropriate test methods-

Property	Applicable Test Std.	Test Method	Test Result	Acceptable Property Range.
Hardness	BS 903 Part A26 1969	Normal Test (N)	Hardness IRHD Scale (converted to Shore by approximation)	80-90°A
Tensile	BS 903 Part A2 1989		50,100 & 300% Modulus. tensile strength & Elongation"@ racture	50% Strain: 3.6-4 .6MPa 100% Strain: 5-8MPa 300% Strain: 8- I 6MPa: Modulus: 40-50MPa Elong: 600-800%
Compression	1S0 77431989 (E)		Compression Modulus @10% Strain	Modulus: 10-20MPa
Tear	BS 903 Parr A3 1982	Method A	Tear Strength	Minimum value of 25KN/m
Shear	0S 2782 Part A3 1987	Method B	Shear Modulus @ 10% S rain	Modulus: 4-8MPa
Compression set @ 23*C	BS 903 Part A6 1989	Methods A and Bat 23°C	Compression set @ Cons ant Strain (25%)	Maximum set: < 20%

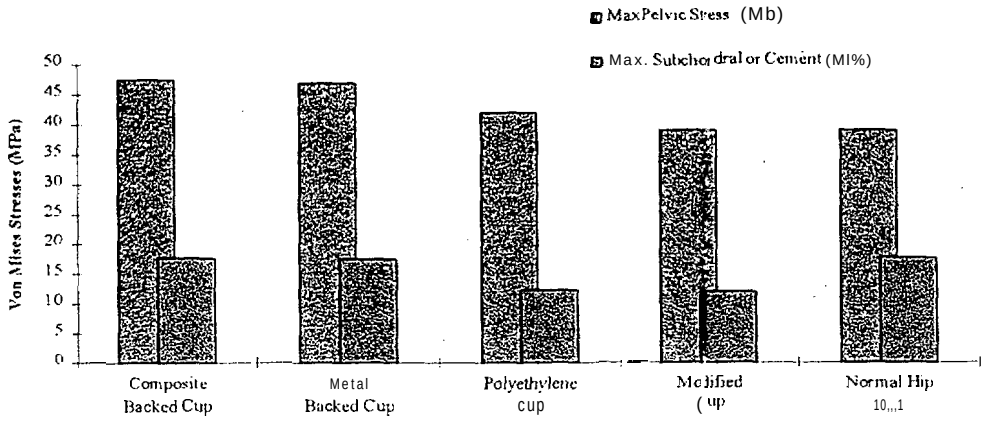

Figure 3: Maximum Von Mises stresses in the Pelvic Acetabular region and Cement or Subchondral Bone

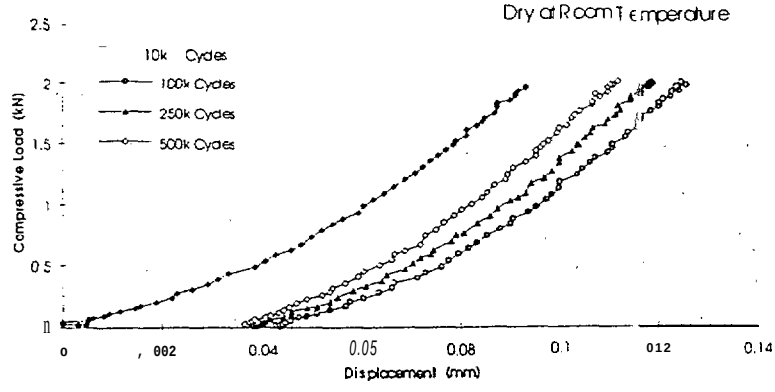

Figure 4: Dynamic Loading of Tecothane1095 "in - situ" Dry at Room Temperature.

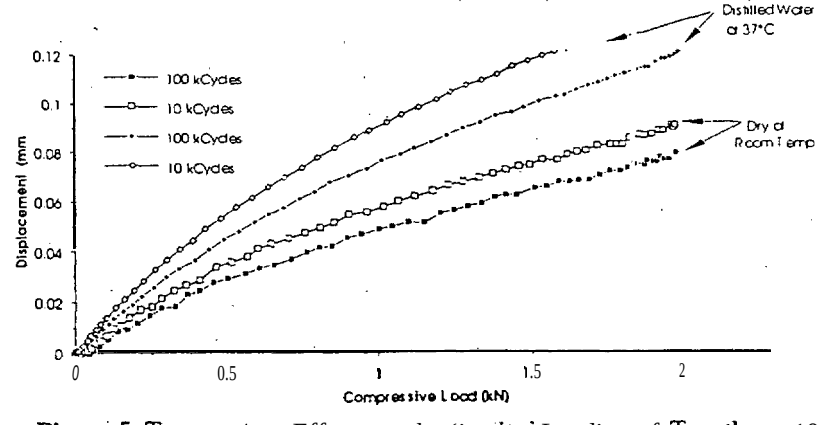

Figure 5: Temperature Effects on the 'in situ' Loading of Tecothane 1095.

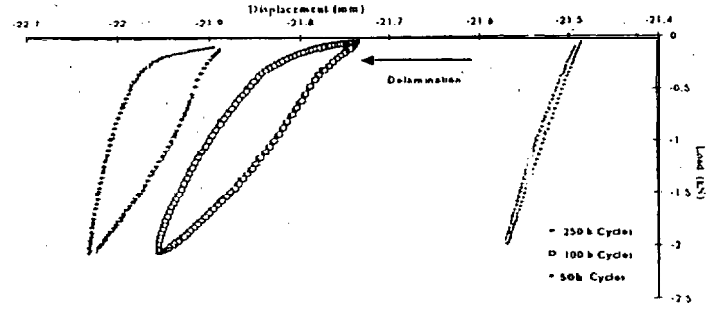

. Figure 6: Fatigue of Tecothane1095 in Ringers Solution at 37°C

Table 2: Fatigue response of polyurethane elastomers at two different loading frequencies.

(A) **Samples loaded to** -2.5 **MPa at** 1.5 Hz.

Cycles	Peak Modulus (MPa)			Energy Dissipated per Cycle (J/Kg)		
	T1085	T1095	E5714F1	'11085	T1095	E5714F1
1×10^4	22.5	46 (38.5')	42.2		4.3 (13.5')	4.9
1×10^5		46 (39.1')	42.2	5.4	5.8 (9.3+)	4.2
2.5×10^5		,47 (40.3+)	42.4	5.5	5.8 (8.9')	3.6
5 X 1 0 5		-- (--)	43.1	3 . 9		2.8

(B) Samples loaded to - 2 . 5 MPa at 10Hz.

Cycles	Peak Modulus (MPa)			Energy Dissipated per Cycle (J/Kg)		
	T1085	T1095	E5714F	T1085	T1095	E5714F1
1×10^4		30.1 (35.2')	39.4		25.1 (24. 1")	12.0
1×10^5		**31.6 (36.7")**	**39.1**		**21.0 (22.2")**	**11.1**
2.5×10^5		**30.5 (39.1")**	**40.3**		**15.2 (20.1")**	**10.8**
5×10^5		**39.7 (39.7)**	**41.7**		**11.0 (19.4")**	**10.5**

*Irradiated samples with a dose of 5.0MRads tested dry. +Samples tested after immersion at Ringer's Solution at 37-C.

Table 3: Baseline compositions (in weight percents) for the three metallurgical powders.

Material	C	Cr	Ni	Mo	Si	Mn	Fe	Co	Al	V	Ti
316L	**0.03**	**17.0**	**12.0**	**2.5**	1.0	2.0	Bal	-	-	-	-
Co-29Cr-6Mo	**0.4**	**29.0**	**2.5**	**6.0**	-	1.0	1	Bal	-	-	-
Ti-6Al-4V	**0.1**	-	-	-	-	-	0.3	-	6.0	4.0	Bal

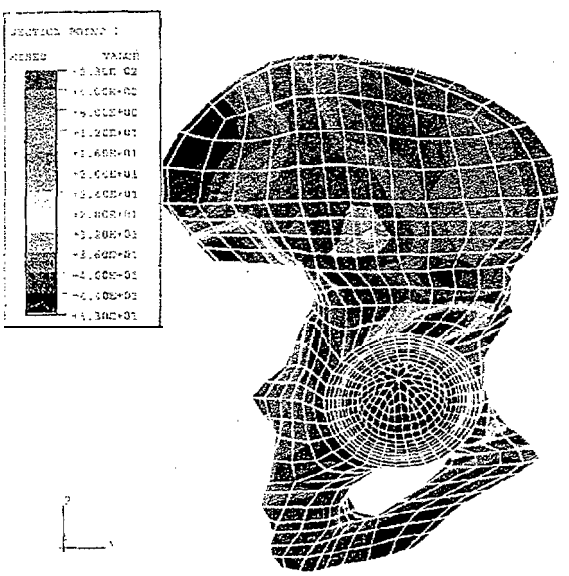

Figure 1: FE stress analysis of a 3-D hemi-pelvis showing the stresses after implantation of a carbon fibre reinforced polymer cup containing a compliant layer.

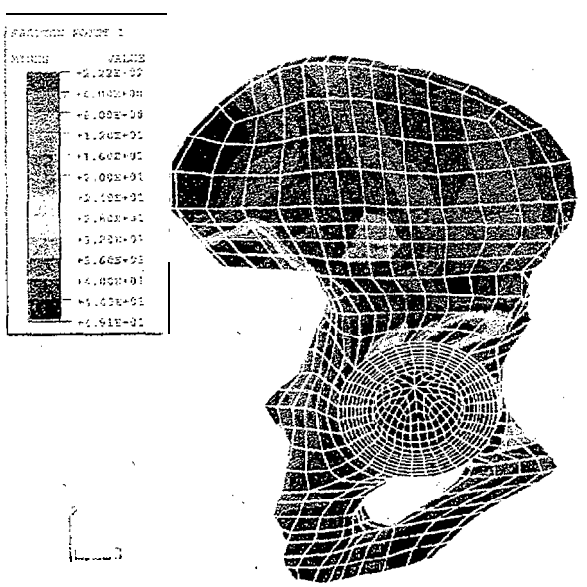

Figure 2: FE stress analysis of a 3-D hemi-pelvis showing natural level of stresses after implantation of a mixec polyurethane layer backed cup,

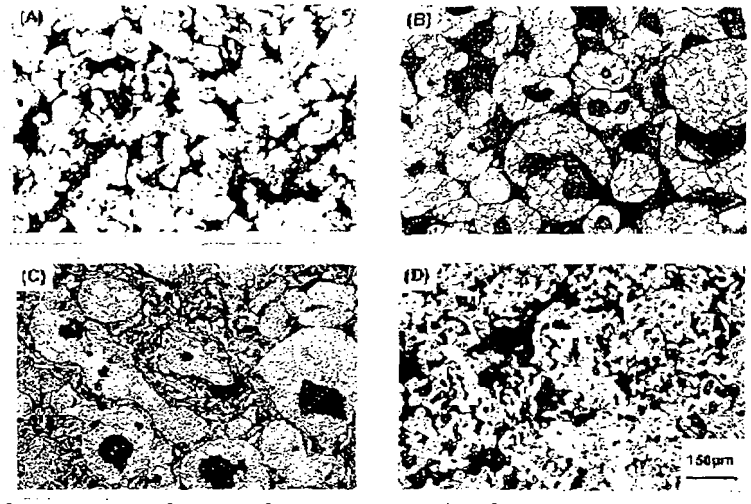

Figure 7: Optical micrographs showing the pore structure in the coarse porosity samples (> 300/. total porosity) for (A) vacuum sintered316L stainless steel, (B) vacuum sintered water atomised. Co-29Cr-6Mo, (c) argon sintered bimodal Co-29Cr-6Mo, (D) vacuum sintered and un-nitrided Ti-6Al-4V.

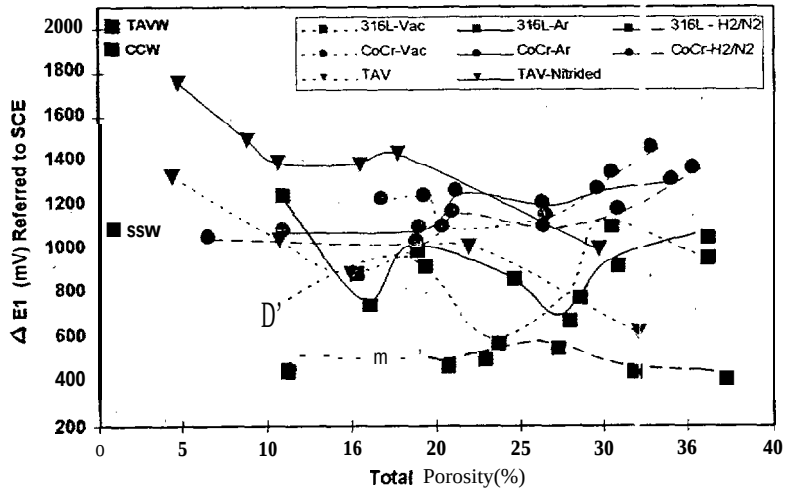

Figure 8: Total porosity versus ΔE comparing the stability of the passive film for316L stainless steels, bimodal Co-29Cr-6Mo and Ti-6Al-4V alloys sintered in various atmospheres. (Water atomised Co-29Cr-6Mo alloys have been omitted for clarity).

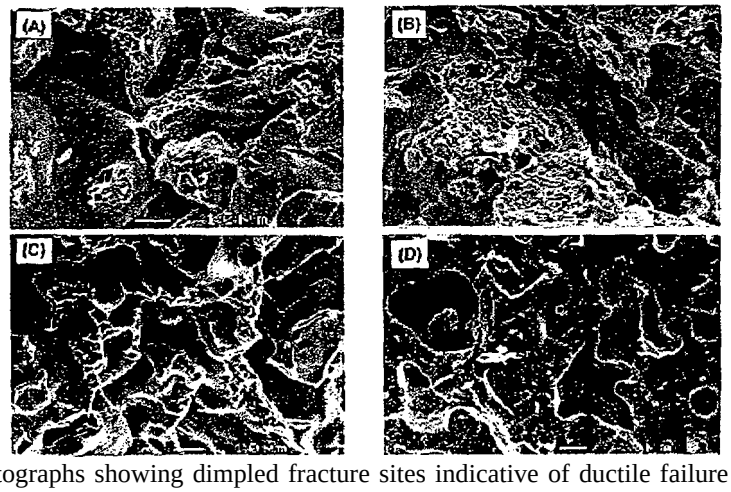

Figure 9: SEM fractographs showing dimpled fracture sites indicative of ductile failure in the coarse porosity samples for vacuum sintered (A) 316L stainless steel, (B) bimodal Co-29Cr-6Mo, (C) un-nitrided Ti-6Al-4V and (D) transcrystalline cleavage fracture in nitrided Ti-6Al-4V.

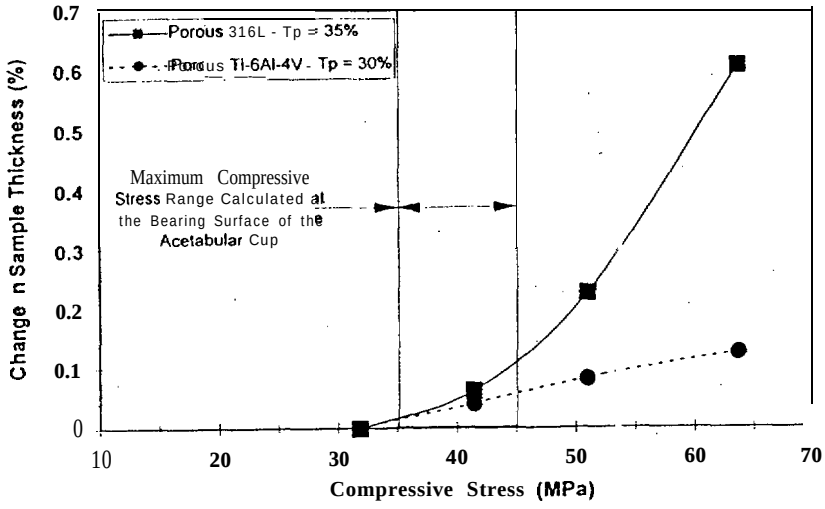

Figure 10: Stress-deflection curves of 3 16L stainless steels and Ti-6Al-4V alloy indicating that pore collapse was possible in the compressive stress range calculated by FE at the bearing surface for conventional acetabular cups.

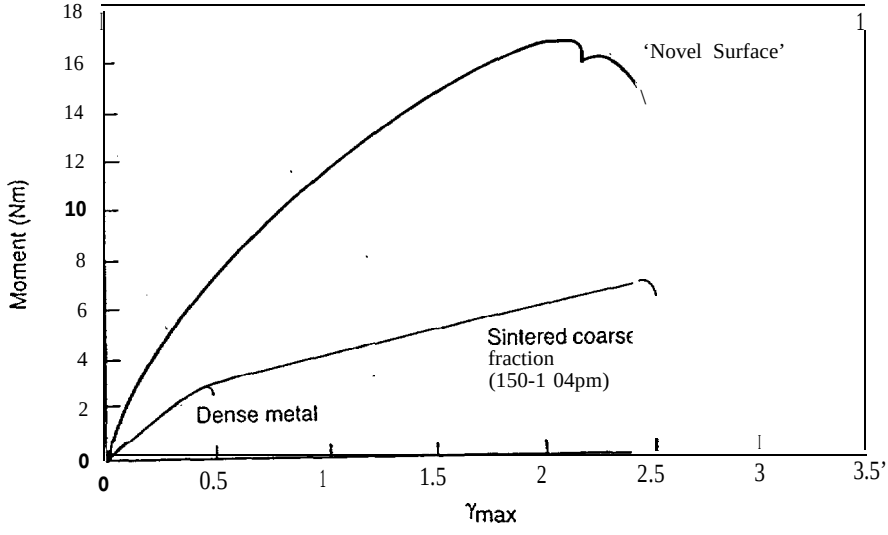

Figure 11: Comparison of torsional moment-shear strain curves of Hewn medicas "novel surface", sintered porous stainless steel (porosity 30°/0) and dense metal joints (grit blasted) using Tecothane 1085A.

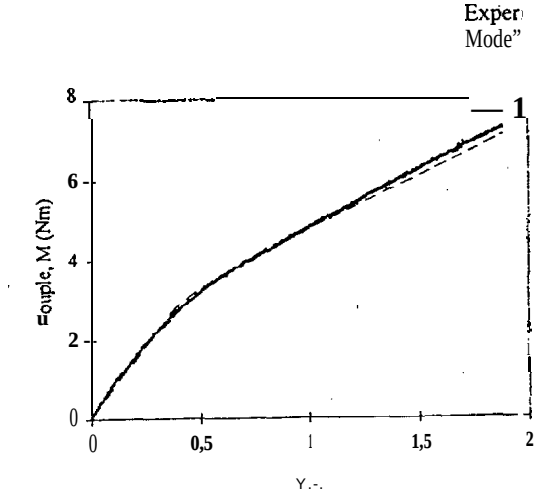

Figure. 12: Comparison between experimental and model; moment-shear strain curves for Tecothane 1085A + sintered 3 16L stainless steel cyt inders of particle fraction 152-104pm. (Model parameters G = 4.8MPa, $\tilde{G}$ = 1.7MPa, y_c = 0.33).

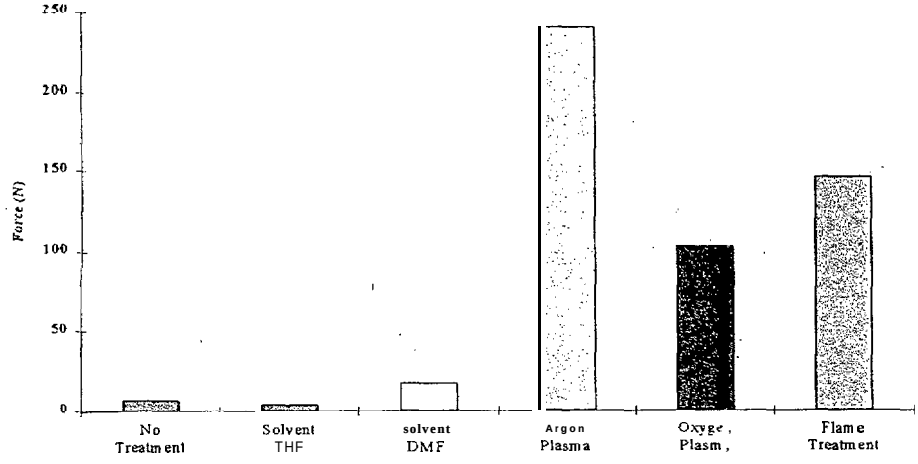

Figure 13: Effect of different surface treatments on the Bond Strength of APC2/PU Joints.

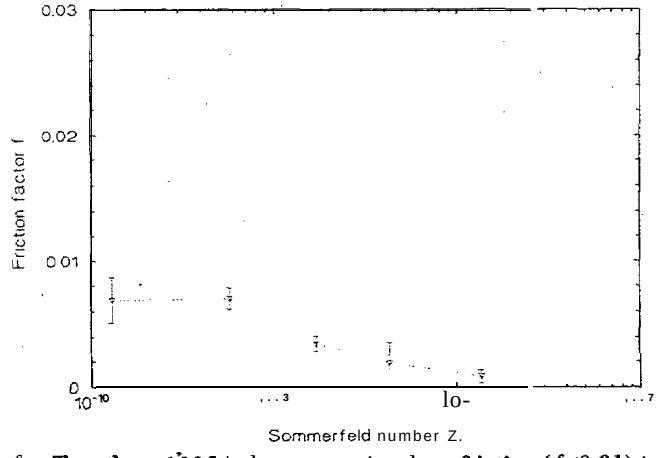

Figure 14: Stribeck curve for Tecothane 1095A demonstrating low friction (f<0.01) indicative of near fluid film lubrication.

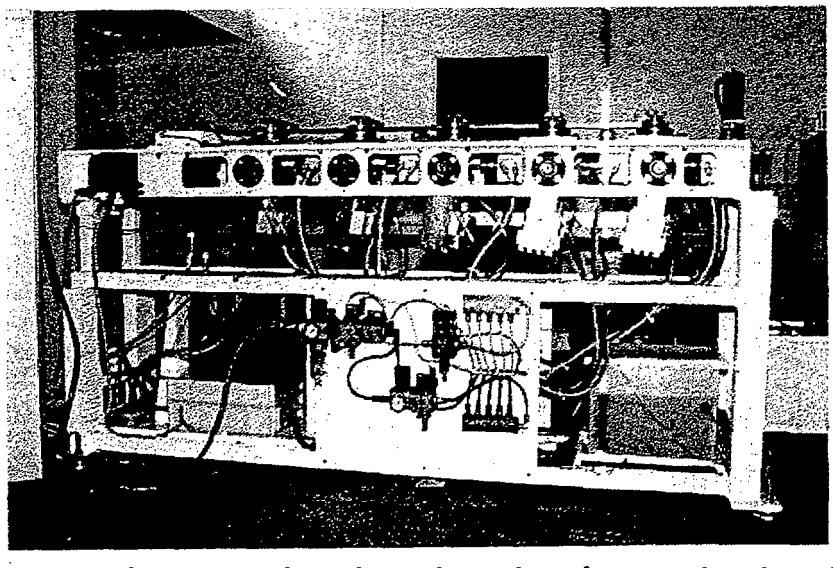

Figure 15: **The** five station hip joint simulator, designed to evaluate the wear and mechanical integrity of the prototype acetabular cups.

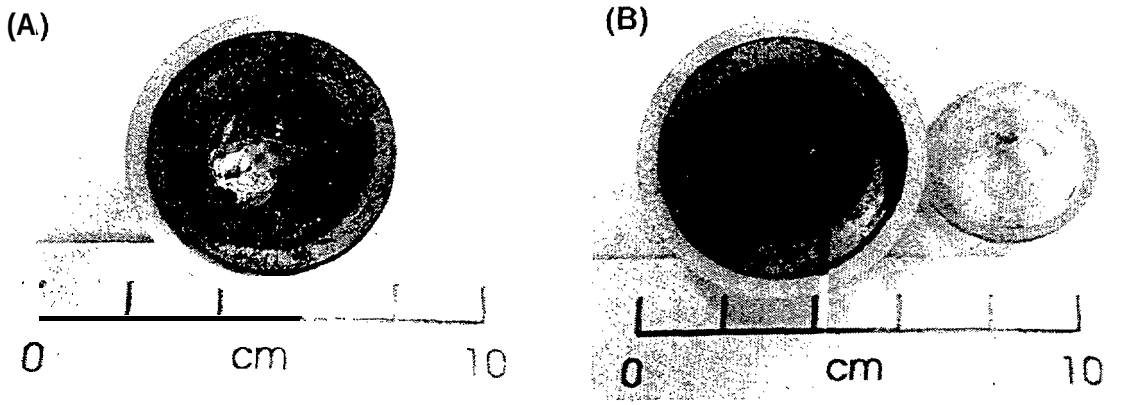

Figure 16: Porous sintered 3 16L stainless steel cups containing (A) Tecotha ne 1095A' after 0.637 million cycles and (B) Tecothane 1085A cup, after 0.054 'million cycles. Note the comple :e detachment of the layer from the backing of cup B.